CrystEngComm

Accepted Manuscript

ROYAL SOCIETY OF CHEMISTRY

www.rsc.org/crystengcomm

CrystEngComm

Cite this: DOI: 10.1039/c0xx00000x

www.rsc.org/crystengcomm

HIGHLIGHT

Nanostructured Materials for Applications in Surface Enhanced Raman Scattering

Xiaochun Chen[b], Changlong Jiang[a]*, and Shaoming Yu[b]*

Received (in XXX, XXX) Xth XXXXXXXXX 20XX, Accepted Xth XXXXXXXXX 20XX

DOI: 10.1039/b000000x

Surface enhanced Raman Scattering (SERS) spectroscopy has become one of the most widely pursued spectroscopic tools for the powerful and extremely sensitive analytical technique with applications in chemical production, biochemistry, and environmental monitoring owing to its integration of unique spectroscopic fingerprint, high sensitivity, and non-destructive data acquisition. The key obstacle for the application of SERS-based sensors is the lack of robust and simple fabrication strategies for renewable SERS substrates with huge and stable Raman enhancement. The rational design of SERS sensors with defined physical and chemical properties is vital for successful applications in many analytical fields. This highlight summarizes current advances on the design and the employment of nanostructured materials in SERS substrates especially from the point of dimensional view. We will then talk about synthesis methods and the novel properties of these nanostructured materials with their potential applications in SERS.

1. Introduction

As a versatile analytical technique, Raman spectroscopy can provide vibrational fingerprints from chemical and biological materials, which can be used to determine chemical species and quantify the level accurately. However, the non-resonance Raman effect is very weak and typically only 1 in 10^{6-8} photons undergo an inelastic light scattering event, which limited use of this potentially analytical technique. The discovery of surface-enhanced Raman scattering (SERS) nearly 40 years ago, the dramatic enhancement of the intensity of the vibrational spectra from molecules located near surfaces of nanostructures when these are illuminated and surface plasmons are excited,[1-5] opened a new avenue for the wider applications of Raman spectroscopy in many different fields.[6-18]

Nanostructured materials have been used as SERS-active materials because of the remarkable novel physical and chemical properties as well as the potential application in sensing. The key obstacle for the application of SERS-based sensors is the lack of robust and simple fabrication strategies for renewable SERS substrates with huge and stable Raman enhancement. Common SERS substrates, such as roughed metallic surfaces and colloidal metal nanoparticles, can provide significant SERS enhancement, however, the highly ordered SERS substrates with reproducible and defined geometries are more effective for routine measurement of trace-level analytes. With the help of modern nanotechnology to control nanoscale structures and materials, much progress has been recently made. Many researches had proved that the plasmon resonance, electromagnetic field enhancement, and hence the SERS enhancement critically depends upon the surface state, shape, size, size distribution, and essence of the metal nanostructures. The distance dependence of the enhancement, namely the arrangement of analyte molecules and metal surfaces or mutual arrangement of adjacent metal nanostructures, is another important factor on the SERS effect.

The rational design of SERS sensors with defined physical and chemical properties is vital for successful applications in many analytical fields. This highlight summarizes current advances on the design and the employment of nanostructured materials in SERS substrates especially from the point of dimensional view. We will first introduce the enhancement mechanism of SERS and the nanostructured materials for SERS. Next, we will discuss recent progress on the fabrication of SERS-active materials with four aspects: noble metal nanoparticles (0D), one dimensional (1D) nanostructures, two dimensional (2D) nanostructures and three dimensional (3D) nanostructures. We will then talk about synthesis methods and the novel properties of these nanostructured materials with their potential applications in SERS.

1.1 Enhancement Mechanism of SERS

For most molecules, Raman scattering is a very weak effect, because the Raman scattering cross section is extremely small. Typical Raman cross section are between 10^{-30}-10^{-25} cm^2 per molecule, and the strong effect occurs only under favorable resonance Raman conditions when the excitation light matches the related electronic transition energy in the molecule.[3, 4, 19] Therefore, the low strength of Raman signals and the inherent lack of sensitivity hinder the use of this potentially very powerful technique.[7] In 1974, Fleischmann and colleagues reported the first measurement of a surface Raman spectrum from pyridine adsorbed on an electrochemically roughened silver electrode when they pioneering applying Raman spectroscopy to the in situ study of electrode surfaces.[7, 10, 11, 20-22] In 1977, Jeanmaire and Van Duyne found that the magnitude of the Raman scattering signal can be greatly enhanced when the scatterer is placed on or near a roughened noble-metal surface.[8, 12, 23, 24] This effect was later called surface-enhanced Raman scattering, and signal levels observed in SERS are typically several orders of magnitude higher than those in conventional Raman scattering.[2] Therefore, the discovery of SERS had promoted a worldwide effort to explore its origins, maximize it, and harness its potential in many fields.

Although the mechanism of SERS enhancement remains an active research topic, it is currently widely accepted that the SERS enhancement are originated by electromagnetic and chemical enhancements, in which the former is responsible for the major portion of SERS enhancement.[2, 6-8, 10, 13, 25-28] Electromagnetic field enhancement depends on the resonance process between surface plasmons and excitation fields, and strong electromagnetic fields are generated at the surface of a nanoparticle adsorbed by a molecule when the localized surface plasmon resonance (LSPR) of the nanoparticle is excited by visible light.[2, 7, 8, 10, 25, 26, 28-33] In sharp contrast, the chemical effect can be attributed to the interaction of the adsorbed molecules with the metal surface, and a charge transfer resonances state is occurred between the metal and adsorbed molecules.[2, 7, 8, 10, 13, 22, 25, 26] The molecule must be directly adsorbed to the roughened surface to experience the chemical enhancement since it is site-specific and analyte-dependent.[8] For electromagnetic enhancement, metals can be considered as the plasma of electrons composed of polarizable, free electrons, and a positive ion core. Interaction of the electromagnetic wave with a metal causes the free electrons to coherently oscillate at the plasmon frequence against the immobile positive ion lattice. When electromagnetic radiation with the same frequency is incident upon the nanostructure, the electric field of the radiation drives the electrons into collective oscillation.[2,8]

1.2 Nanostructured Materials for SERS

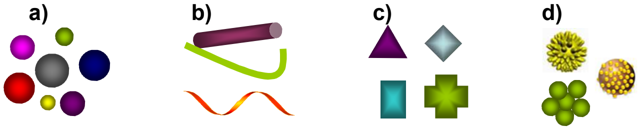

Figure 1. Schematic images of the different dimensional nanostructures for SERS applications: (a) nanoparticles, (b) one dimensional (1D) nanostructures, (c) two dimensional (2D) nanostructures, and (d) three dimensional (3D) nanostructures.

Nanostructured materials often exhibit novel chemical and physical properties that are radically different from their bulk counterparts.[25] Due to the remarkable properties and the potential application in SERS, various kinds of metal nanostructured materials, including noble metal nanoparticle, one dimensional (1D) nanostructures, two dimensional (2D) nanostructures, and three dimensional (3D) nanostructures, have been reported to give rise to large SERS enhancement (Figure 1). While there are several aspects that affect the magnitude of the SERS enhancement factor, the characteristics of nanostructured materials, such as their size distribution, geometry, chemical composition, and surface chemistry can influence the Raman enhancement ability.[6, 24, 34]

Electromagnetic field enhancement depends on the resonance process between plasmons and excited fields, and the nanostructured materials used for the SERS must be smaller than the wavelength of the exciting electromagnetic radiation.[2, 35] Among them, metallic materials of gold and silver are the most commonly used SERS active materials, which can provide large enhancement.[1-3, 6, 10, 36-42] It has been proved that SERS active materials should be in the range of 5-100 nm while the strongest SERS effects are usually observed from nanoparticles in size of 20-70 nm.[20] Additionally, the nanoparticle should not be too small than 5 nm to prevent it from deviating from the pseudo bulk plasmon behavior and exhibiting quantum effects.[2] For nanoparticles that are smaller than 5 nm, the electronic scattering at the surface plays a major role, resulting in the depletion of the electrical conductivity, leading to poor polarizability of the particle and hence weakening the plasmon resonance quality and SERS effect.

LSPR, which is dependent on several features of the nanostructured materials, such as size, shape, composition, and crystallinity, of which size and shape are more significant, [25, 26, 30, 32, 34] is of tremendous importance to their applications in SERS.[34] The LSPR of the nanostructured materials can be excited to produce highly intense localized electromagnetic fields, which are able to dramatically enhance the Raman scattering cross sections of molecules in their proximity. Surface plasmons of metallic nanostructures are very sensitive to morphologies and dielectric environments of nanostructures.[43] Particularly, strongly enhanced and inhomogeneous localized electromagnetic fields at sharp edges, junctions, and narrow gaps of nanostructures have been observed experimentally and verified by computational simulations. These localized electromagnetic fields are known as “hot spots”.[6, 8, 22, 30, 43, 44] In order to get high SERS enhancement factors, one must increase the occurrence rate of SERS hot spots. Recently, various kinds of nanostructures with rich sharp edges, junctions and narrow gaps, such as nanostars[45-47], nanodisks[48, 49], and nanoflowers,[50-56] have been prepared for SERS substrates. Thus, shape control of the nanostructured materials has been a hot topic in the SERS research. Most of the shape controlled syntheses involve the reduction of salt precursors or thermal decomposition of organometallic compounds in the presence of organic surfactants, polymers, biomacromolecules, and coordinating ligands, and sometimes with the mediation of ionic species, have been developed and employed to control the shape of nanostructured materials.

2. Nanoparticles

Noble metal nanoparticles (NPs) including gold NPs, silver NPs and copper NPs are commonly used as SERS-active materials because of their excellent plasmonic properties. Single nanoparticles, composite nanoparticles and nanoparticle clusters are the most widely used noble metal NPs for SERS. These metal NPs provide a localized surface plasmon resonance leading to a large local electromagnetic field.[34, 35] Such an electromagnetic field is capable of enhancing Raman scattering signals, and has been used for enhancing the performance in the function of enhanced Raman scattering. Noble metal NPs with different size, shapes, and aspect ratios would exhibit distinct LSPR properties and dramatically enhance the SERS effect.[43]

2.1 Single Nanoparticles

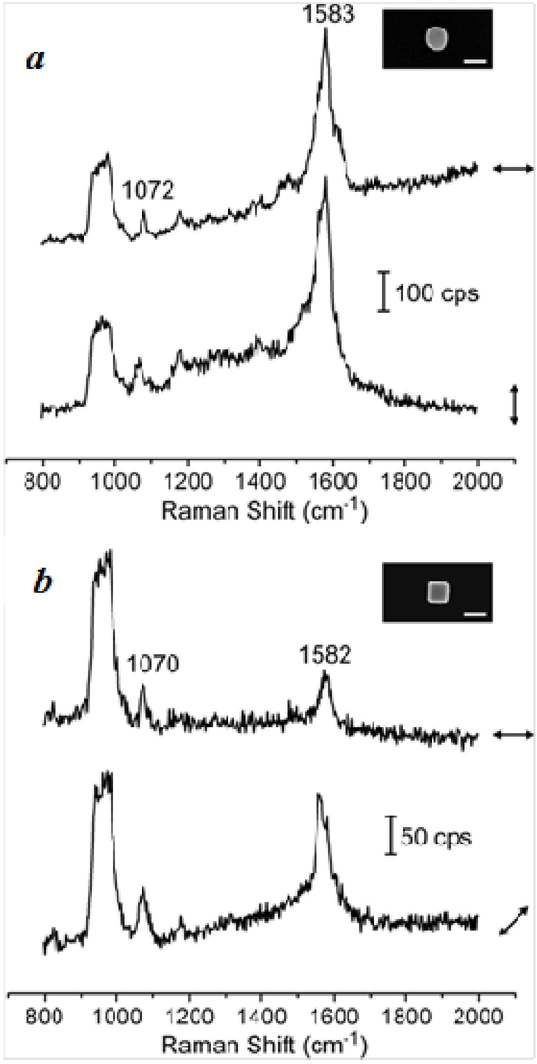

Figure 2. SERS spectra of 4-methylbenzenethiol (4-MBT) from an individual silver nanosphere (a) and nanocube (b). Each arrow indicates the laser polarization direction relative to the nanosphere or nanocube in the SEM image. For the nanosphere, no significant variation was observed for the spectra taken at different polarization directions. For the nanocube, the SERS signals were more strongly enhanced when the laser was polarized along a face diagonal (bottom trace in B). The insets show SEM images of the probed nanosphere and nanocube. The scale bars in the insets correspond to 100 nm. (reprinted with permission from ref. 43. Copyright 2010)

Based on the EM enhancement theory, SERS intensity is dependent on the resonance frequency of the noble metal substrate. The plasmon resonance frequencies depend on the size of NPs, especially for Ag and Au NPs. For instance, the plasmon band of Ag NPs exists at 406 nm for the size of 22.8 nm while NPs in a diameter of 37.8-nm show a peak at 428 nm with a significant red shift.[57] It is also well known the field enhancement is greatest when the plasmon frequency of NPs is in resonance with the laser radiation. Xia and co-workers reported a systematic study of the SERS enhancement from sharp and truncated Ag nanocubes with a size ranging from 60 to 100 nm. The results indicated higher SERS enhancement for particles of large size (90 and 100 nm), which can be attributed to the overlap between the laser source and plasmon resonance band of the NPs.[58]

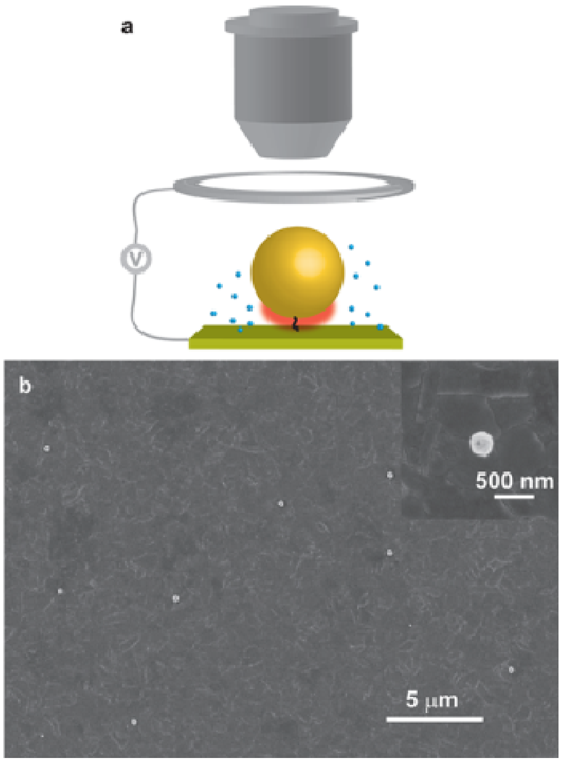

Figure 3. (a) Schematic showing the configuration of the AuNP probe-molecule-vanadium-oxide junction and the in situ electrochemical SERS measurement scheme. (b) A representative SEM image showing dispersed single AuNPs on the vanadium oxide electrode. The inset shows a magnified view of a typical single AuNP. (reprinted with permission from ref. 61. Copyright 2014)

It is clear that the LSPR of single nanoparticle is sensitive to the composition, size, shape, and local dielectric. Under ensemble measurements, spectral, structural, and functional properties of single particle may be hidden.[35] In order to better understand the SERS property of single particle, recent researches have shifted attentions toward single nanoparticle measurements.[35] Thus, different characterization techniques have been employed to single nanoparticle measurements.[59, 60] For instance, Blaber M.G and co-workers had used high-throughput wide-field single nanoparticle spectroscopy and TEM to determine the optical and structural properties of single nanoparticle.[35] Some researches on single nanoparticles suggested the dependency of SERS enhancement factors (EFs) on laser polarization. Figure 3 shows a comparison study of the polarization dependency for silver nanocubes and nanospheres.[43] For the nanosphere (Figure 2A), due to its isotropic nature, the surface plasmon will oscillate similarly in all directions. Thus, there is no dependence on polarization. Figure 2B shows the SERS spectra of 4-methylbenzenethiol (4-MBT) on silver nanocubes with two different laser polarizations. In this case, the largest SERS EF is recorded when the nanocube is oriented with a face diagonal axis parallel to the laser polarization, in contrast to polarization parallel to one of the cube's edges. So it can be concluded that the strongest SERS intensities of nanoparticles with sharp features can be seen when the polarization is along an axis that connects two sharp features.

Gold and silver nanoparticles are the most widely used Raman enhancing materials, and they have many advantages, including having an easily controlled size distribution, long-term stability, and significantly high biocompatibility. Typical gold NPs are synthesized by the citrate-reduction procedure, as originally reported by Frens,[6] and the silver NPs are usually prepared by the reduction of $AgNO_3$ either with sodium citrate acid at boiling condition or with hydroxylamine hydrochloride at room temperature. Furthermore, the combination of SERS transduced by single NP probes with electrochemical processes can be used to probe interfacial reactions. Li and co-workers used the single nanoparticle probes to see real-time molecular changes correlated to electrochemically modulated ion-intercalation in metal-oxide electrodes (Figure 3). Using SERS transduced by single NP probes, they observed that the Raman frequencies and spectral intensities of the adsorbed molecules vary on cycling the electrochemical potential on a vanadium-oxide electrode.[61]

2.2 Composited Nanoparticles

The composited nanoparticles, comprising two or more different components, have attracted much attention due to their unique composition-dependent physicochemical properties and multiple functionalities, which are not usually achievable in single nanoparticle.[62-68] Recently, noble metal NPs have been combined with other NPs to make composites capable of SERS sensing and some novel properties. Given the beneficial properties of metal NPs as well as other NPs for SERS, the NP composites should be attractive for use as SERS active materials.[65]

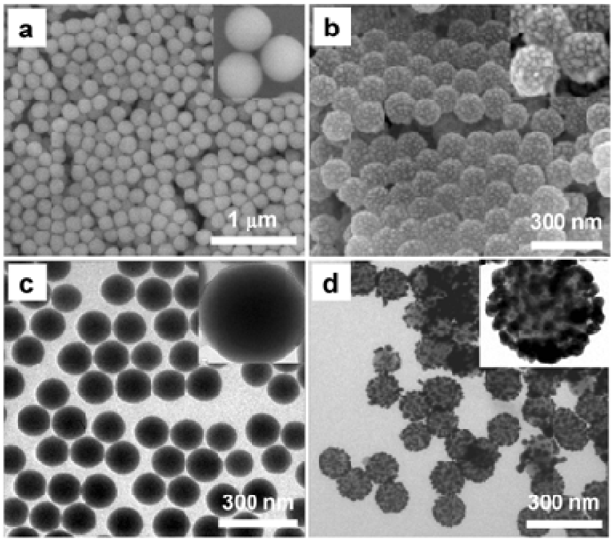

Figure 4. Typical SEM and TEM images of the SiO_2@Ag nanocomposites. (a) The SEM image of the SiO_2 nanospheres, inserted is the higher magnification image of the nanospheres; (b) The SEM image of the Ag nanocontacts loading onto the SiO_2 nanospheres, inserted is the higher magnification image; (c) The TEM image of the SiO_2 nanospheres, inserted is the higher magnification image of the nanospheres; (d) The TEM image of the Ag nanocontacts loading onto the SiO_2 nanospheres, inserted is the higher magnification image. (reprinted with permission from ref. 64. Copyright 2014)

Inorganic nanostructures with various shapes and sizes, including metal, metal oxide, and semiconductor nanocrystals, are usually composited with metal NPs for SERS.[63] Han Y. B. and co-workers have developed SiO_2@Ag nanocomposites as an effective SERS detection platform through in situ loading Ag nanocontacts onto the SiO_2 nanospheres, the well-designed and uniform nanocomposities provide highly enhanced effect for the tremendous SERS signal amplification (Figure 4). The huge enhanced effect might originate from the hot spots generated from the nanocontacts among the silver nanoparticles loaded onto the silica nanosphere, and also possibly from the nanogaps among the neighboring silver nanoparticles between the two silica nanospheres.[64] It is well-known that graphene can adsorb or link with various organic molecules owing to its unique surface structure, which makes it an attractive candidate for selective SERS sensing.[39, 65] Our group designed a SERS-active substrate based on a graphene oxide embedded sandwich nanostructure for ultrasensitive Raman signal readout, which can dramatically enhance the Raman signals of analytes because of having plenty of hot spots on their surfaces and the unique structure of the graphene oxide sheets. The sandwiched composite SERS platform can be applied to detect the pesticide thiram in commercial grape juice with a detection limit of as low as 0.03 ppm.[39] Furthermore, a reduced graphene oxide-Ag nanoparticle (RGO-AgNP) composite had been designed by Murphy S and co-workers for SERS application. Complexation between 5,10,15,20-tetrakis (1-methyl-4-pyridinio) porphyrin tetra (p-toluene-sulfonate) (TMPyP) porphyrin was used as target molecule.[65] The RGO-Ag NP composite exhibits greater SERS signal enhancement for target molecule that complexed with RGO.

In addition to inorganic nanostructures, polymer-metal NCs have also been developed as efficient SERS substrates.[63, 67, 69, 70] Because of their amphiphilic nature, Pluronic copolymers are expected to reversibly interact with both hydrophilic and hydrophobic compounds in aqueous solution.[71] Therefore, Pluronics can be potentially exploited to control the selectivity of metal nanoparticle probes toward analytes. Abdullin T.I. and co-workers prepared composite nanoparticles composed of AuNPs and AgNPs covered with a thin Pluronic copolymer shell.[71] The copolymer coated AgNPs show higher SERS activity than the counterparts prepared with AuNPs. Among the prepared composites, the AgNPs modified with Pluronic F127 containing extended poly(propylene oxide) and poly(ethylene oxide) blocks exhibit maximal Raman activity using rhodamine 6G (Rh6G) with an enhancement of 9.04×10^6.

2.3 Nanoparticle Cluster

SERS signals achieved from nanoparticle clusters can be very strong because of the so-called hot spots generated within the nanoparticle gaps.[23, 24, 44, 72, 73] Nanoparticle clusters of noble metals, especially gold and silver, are emerging materials with unique SERS properties.[69] Typically, enhancement observed from nanoparticle clusters is many orders of magnitude greater than that of single nanoparticles, which can be attributed to plasmon coupling between adjacent nanoparticles among the clusters, resulting in huge electromagnetic field enhancements at junction sites or SERS hot spots.[73] Salt-induced aggregation is the most commonly used method. To obtain SERS active materials with the desired extent of aggregation, the amount of salt added should be precisely controlled.[75] Moreover, organic reagents-induced aggregation is a novel technique. Sun L. and co-workers synthesized the silver nanoparticle clusters by adding different amounts of ethanol to cetyltrimethylammonium bromide (CTAB) capped silver nanoparticles, which is highly efficient for SERS.[71] Two common probe molecules, Rhodamine 6G (R6G) and 4-aminothiophenol (4-ATP) were used for testing the SERS activity on the silver nanoparticle clusters at very low concentrations. It was found that the SERS enhancement ability is dependent on the ethanol volume used, and the SERS enhancement factors of 4-ATP were estimated to be as large as 8.1×10^8. In the aggregation process, polymers are usually applied to quench the aggregation process by forming a shell on the particle's surface. Another novel method to form nanoclusters is the dye-induced aggregation. Upon adsorption of Raman reporters, the capping agent (such as citrate) on the surface of metal NPs is replaced, which decreases the electrostatic repulsion between particles and therefore induces the formation of closely adjacent NPs and further the nanoparticle clusters.[6, 77]

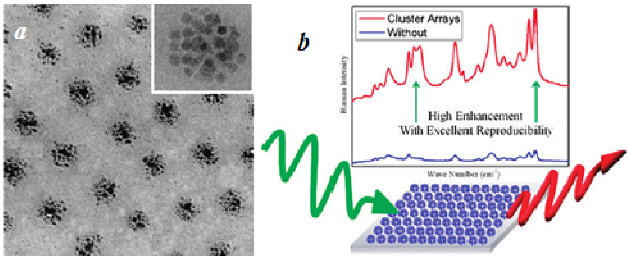

Figure 5. TEM image (a) and schematic illustration of the ultrahigh-density array of silver nanoclusters for SERS substrate (b). (reprinted with permission from ref. 79. Copyright 2012)

Recently, a few groups began to study the correlation between SERS intensity and nanoparticle cluster size.[44, 73, 78] Wustholz K.L. et al. had studied the SERS enhancement provided by individual NP clusters with varying size.[78] They had employed field flow fractionation to control over the NP aggregations and stabilized the resulting clusters by individually encasing them in SiO_2 shells, and they discovered that there is not necessarily an increase in SERS enhancement with the cluster size. These results showed that a NP dimer can provide SERS intensities as high as that of a NP heptamer, with the enhancement much more dependent on the size of the interparticle gap. In order to control the variations in SERS intensities, a type of NP probe typically has a NP core protected by a coating of polyethylene glycol (PEG), which could control the gap distance between the Au-NP cores upon aggregation, leading to smaller variations in SERS intensities. In Shaw C.P. and co-workers' report, they investigated a statistical approach to the quantification of SERS from the probe clusters.[44] The investigation began by considering multiple biotinylated surfaces that had been exposed to pegylated NPs (designed for biological SERS mapping) functionalized with streptavidin (defined as SERS probes). The surfaces were imaged with a scanning electron microscope and SERS-mapped with a Raman microscope. Statistical distributions of the SERS probe clusters and mapped SERS intensities on the surfaces were developed. It was found that there was a smooth polynomial relationship between SERS intensity and probe cluster size. In another research, Kim and co-workers introduced a simple but robust method to fabricate an ultrahigh-density array of silver nanoclusters for SERS substrate with high sensitivity and excellent reproducibility at a very large area (wafer scale) based on a copolymer micelles.[79] They systematically controlled the gap distance between two neighboring silver nanoclusters ranging from 8 to 61 nm, while the diameter of each silver nanocluster was kept nearly constant (~25 nm). Fabricated SERS substrate with a gap distance of 8 nm showed very high signal intensity with a SERS enhancement factor as high as 10^8, which is enough to detect a single molecule, and excellent reproducibility (less than ±5%) of the signal intensity (Figure 5). This is because of the uniform size and gap distance of silver nanoclusters in a large area.

3. One Dimensional Nanostructures

Due to the remarkable specific physical and chemical properties as well as the potential application, 1D nanomaterials, such as nanowires[22, 80-86], nanofibers[87, 88], nanobelts[89-94], nanorods[22, 95-101] and nanotubes[102-114], have attracted great research interests.[115] Nowadays, various types of one 1D nanostructures have been reported to give rise to huge SERS enhancement with the help of nanotechnology. According to the morphology properties, one dimensional nanomaterials can be classified as solid nanocrystals and hollow nanocrystals.[30]

3.1 Solid Nanocrystals

In recent studies, solid nanocrystals have always been used to give rise to the SERS enhancement. Nanorods, nanowires, nanobelts and nanofibers, are the most commonly used one dimensional solid nanocrystals for SERS applications, as discussed below.

3.1.1 Nanorods

Rodlike nanocrystals of metals with tunable optical and electronic properties have been the focus of intensive research due to their size- and shape-dependent properties and potential applications in sensing, catalysis and other fields.[98] Many methods have been employed to the synthesis of nanorods. In Guo S. and co-workers' paper, a polyol method was developed for large-scale synthesis of rectangular silver nanorods in the presence of directing agent and seeds.[92] They applied a liquid-liquid assembly strategy to construct uniform rectangular silver nanorod arrays on a solid substrate which could be used as SERS substrates with high activity, stability, and reproducibility. 4-aminothiophenol (4-ATP) and rhodamine 6G (R6G) were chosen as probe molecules, and the enhancement factors for 4-ATP and R6G should be as large as 5.06×10^4 or much larger than the value of 5.06×10^8, respectively. Besides, Shanmukh S. and co-workers recently used the oblique angle deposition (OAD) method to fabricate a silver nanorod array, which was applied as an extremely sensitive SERS substrate with enhancement factor of greater than 10^8.[115] Liu Y.-J. and co-workers also used the OAD method at various vapor deposition angles to synthesize silver nanorod arrays with different lengths, and the arrays have been studied systematically on their morphologies, optical reflections, and SERS responses.[99] They found that the SERS enhancement factor shows a strong dependence on the nanorod length and deposition angle, decreases nearly monotonically with the increase of the reflectance at SERS excitation wavelength, and the highest SERS enhancement factor can reach up to 10^9. Unlike other Au nanostructures which have one SPR band, gold nanorods have two: a weak transverse band in the visible region with a position that corresponds to electron oscillations along the short axis and a strong longitudinal band in the longer wavelength region that corresponds to electron oscillation along the long axis.[6] The tunable, longitudinal plasmon resonance that can be engineered by changing the aspect ratio has made Au nanorods attracted much attention.

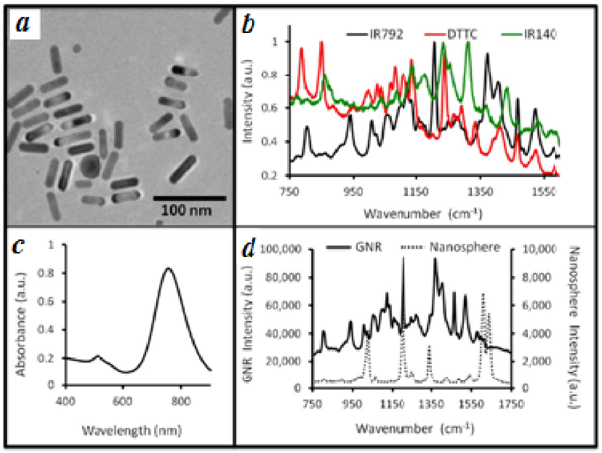

Figure 6. Gold nanorods for photoacoustic (PA) and SERS imaging. (a) TEM image of GNRs shows typical morphology with an aspect ratio of 3.5; (b) After functionalization with different Raman reporter molecules, a unique spectrum is recorded for each type of GNR; (c) The GNRs have both a longitudinal (~760 nm) and an axial (~530 nm) absorbance peak; (d) A comparison of the SERS signal of GNRs (left ordinate) to a similar silica-coated spherical nanoparticle (right ordinate) shows enhanced signaling capacity, but with higher baseline for the GNRs. (reprinted with permission from ref. 116. Copyright 2012)

Au nanorods have been made as Raman scattering probes in sensing applications, such as single molecular, cell and DNA detection. Gambhir S. S. and co-workers developed a gold-based molecular imaging agent that allows presurgical photoacoustic visualization of a tumor for loco-regional staging as well as intraoperative SERS imaging for complete resection of tumor margins.[116] Gold nanorods with higher aspect ratios offered increased *ex vivo* and *in vivo* signal readout (Figure 6). Vigderman L. and co-workers had prepared higher-order penta-branched gold nanorods which contain a uniquely periodic starfruit like morphology.[100] The gold nanorods are synthesized in the presence of silver ions by a seed-mediated approach based on utilizing highly purified pentahedrally twinned gold nanorods as seed particles, and the nanorods exhibit good SERS properties.

3.1.2 Nanowires

Similar to nanorods, electronic and optic properties have made nanowires widely used in sensing applications.[98] Up to now, several methods for the synthesis of nanowires have been developed, including chemical synthesis, electrochemical technique, hydrothermal method, ultraviolet irradiation photodetection technique, DNA template, and polyol process.[86, 98] Chen M. and co-workers had successfully synthesized silver nanowires with diameters of 50−500 nm and lengths up to tens of micrometers via a simple wet chemical route using cuprous oxide nanospheres as a reductant and directional agent.[82] The silver nanowires had been used as the SERS probe with high activity and stability for detecting Rhodamine 6G (R6G) molecules. Mohanty P. et al. reported that single-crystalline free standing Ag nanowires had been synthesized in the vapor phase using a single precursor.[85] This method provided nanowires with a clean surface that can serve as a well-defined and well-characterized SERS-active system, and the SERS effect from a single nanowire showed strong polarization dependence. However, it is obviously that metallic nanowires with smooth longitudinal surfaces can only couple to light weakly due to discrepancy between photon and nanowire plasmon dispersion relations. This problem had been resolved by increasing gaps and sharp edges on longitudinal length of nanowires. Vigderman L. and co-workers synthesized starfruit-shaped penta-branched gold nanowires by seed-mediated approach, which showed 25 times SERS enhancement as compared to its smooth counterpart.[100] Goh M.S. et al. used a chemical etching method to increase the surface roughness of Ag nanowires, targeted at creating more SERS active hot spots along Ag nanowire's longitudinal axis for increased SERS detection sensitivity.[85] They first synthesized silver nanowires by the conventional polyol method and then increased the surface roughness by using a chemical etchant consisting of NH_4OH/H_2O_2. The surfaces of silver nanowires were anisotropically etched off to create miniature "beads on a string" features with increased surface roughness while their crystallinity was preserved throughout and after etching reactions (see Figure 7). The Raman mapping of the single nanowire indicated that the micrometer length longitudinal axis of the etched nanowires exhibited a SERS enhancement factor of about 10^4, while the Ag nanowires only showed limited SERS signals at their tip.

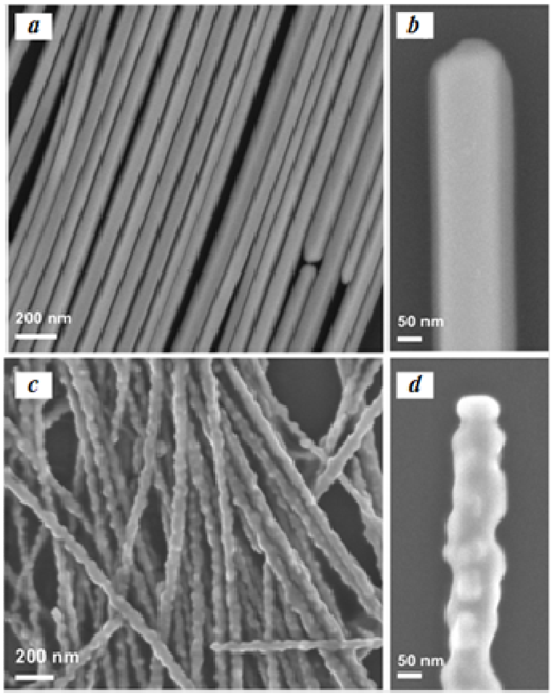

Figure 7. SEM images of (a, b) as-synthesized and (c, d) chemically etched Ag nanowires. (reprinted with permission from ref. 85. Copyright 2012)

3.1.3 Nanobelts

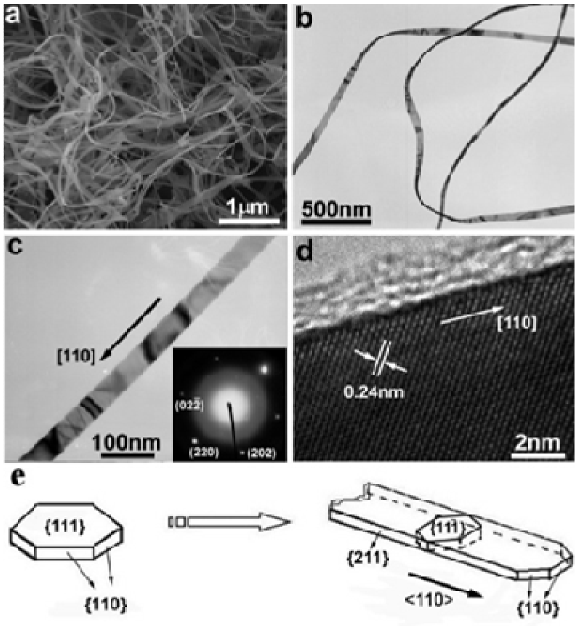

Figure 8. SEM (a), TEM (b,c), and HRTEM (d) images of gold nanobelts obtained at 4 °C. (e) Schematic illustration of the growth direction of gold nanobelts. (Inset) ED pattern corresponding to the whole region of c. (reprinted with permission from ref. 93. Copyright 2008)

Nanobelts are special 1D nanostructures with nearly rectangular cross sections.[91] Because of their unique shape-dependent electrical, mechanical, optical, and chemical properties, many nanobelts, including metals, metal oxides, and metal chalcogenides, have been synthesized.[88-93] It is accepted that the length of the nanobelts is of vital importance for their properties. For instance, the length of the nanobelts will influence the SERS properties, since the different lengths will lead to different surface roughness, which is the key factor for SERS applications.[93] As a member of 1D nanostructures, inorganic nanobelts have attracted much attention since the first report of ZnO nanobelts.[112] Bai J. and co-workers reported a facile low-temperature synthesis of unique silver nanobelts under the direction of poly(acrylic acid) (PAA) in aqueous solution.[91] In Zhao N. and co-workers' report, they had synthesized well-defined gold nanobelts by the reduction of $HAuCl_4$ with ascorbic acid in aqueous mixed solutions of the cationic surfactant cetyltrimethylammonium bromide (CTAB) and the anionic surfactant sodium dodecylsulfonate (SDS).[93] Single-crystalline gold nanobelts grown along the <110> and <211> directions were prepared in mixed CTAB-SDS solutions at 4 and 27 ℃ , respectively (Figure 8). The gold nanobelts were used as the SERS substrate for detecting the p-aminothiophenol (PATP) molecules with high sensitivity. Rayapati Venugopal et al. had successfully fabricated single-crystalline CdSe nanobelts by a chemical vapor deposition (CVD) method assisted with laser ablation.[92] They used surface-enhanced Raman scattering and normal Raman scattering spectroscopies with off- and near-resonant excitations to measure the phonon modes of CdSe nanobelts and bulk powder. A blue-shift of 2.4 cm^{-1} for the longitudinal optical (LO) phonon of CdSe nanobelts, relative to bulk CdSe, is attributed to a lattice contraction in the belt structure. According to Payne C.M. and co-workers, they used the surfactant-directed chemical synthesis to produces uniform nanobelts as well as similar, yet more complex, structures.[88] And nanobelts also form dimers, either because of bifurcation during growth or because of alignment during deposition, that run side by side with sub-10 nm gaps which create large volumes of electromagnetic enhancement for surface-enhanced Raman spectroscopy.

3.2 Hollow Nanocrystals

Comparing to solid nanocrystals, hollow nanocrystals have better sensing properties than solid ones. This is due to the presence of interior and exterior plasmon fields that couple with one another resulting in a much stronger field and the hollow shapes that produce a more evenly distributed plasmonic field.[30] Usually, conventional SERS nanostructured probe are metallic nanostructures, but the most common nanotubes used for SERS are carbon nanotubes.[108-119] Because of the extraordinary electrical, thermal, and mechanical properties, carbon nanotubes have been, concurrently, a topic of extensive research and applications in sensing.[115] Although carbon nanotubes were successfully used for SERS, the combinations with other elements like gold and silver can be anticipated to increase their efficiency as SERS substrates. Sun Y. and co-workers reported that silver nanoparticles can be automatically formed on the surface of one-dimensional carbon nanotubes by e-beam evaporation, leading to a unique structure which was beneficial to the enhancement of local E-field.[118] Then they made the carbon nanotubes cross stacking superaligned. The as-prepared SERS substrate could provide sensitive detection of different organic molecules, especially the detection of ambient explosive vapor with extremely low vapor pressure. Chen Y.-C. and co-workers also prepared a nanostructure of single walled carbon nanotubes decorated with Ag nanoparticles,[113] and Ag nanoparticles were electrochemically deposited on a network of single walled carbon nanotubes. The Ag NPs decorated CNTs exhibit a high SERS enhancement with specific hot spots that allow the observation of a Raman signal from one or a few molecules. Goldberg-Oppenheimer P. and co-workers had made gold functionalized vertically aligned carbon nanotube forests, and a benzenethiol monolayer was used to test the SERS performance of the hybird structures. The absolute enhancement factor is calculated to be about 1.0×10^7.[115]

4. Two Dimensional Nanostructures

Two dimensional (2D) nanostructures have been extensively studied because of their remarkable abilities in sensing properties. As a result, lots of approaches have been employed to fabricate 2D nanostructures such as nanoplates[118-126], nanoprisms[127-133], nanodisks[50, 129-135] and nanostars[47-49]. The peak wavelength and localized surface plasma resonance of these nanostructures are significantly dependent on their morphology, size, interparticle spacing, intrinsic dielectric properties, and local environment ,such as adsorbates.[122] Recently, various types of 2D nanostructures have been reported for SERS applications.

4.1 Nanoplates

Among various shapes, the nanoplates that have sharp corners and edges are supposed to be most active for SERS. In the past decade, a library of strategies for fabricating metal nanoplates has been developed, including photochemical routes, thermal organic synthesis, and seed-mediated, microwave-assisted, and ultrasound-assisted aqueous chemical reduction methods.[119] Zou X. and co-workers synthesized citrate-protected silver nanoplates via a seed-mediated approach, which silver seeds were firstly obtained and then silver nanoplates were prepared by enlarging the small silver seeds in the presence of citrate.[123] The silver nanoplates were served as active SERS substrates with an enhancement factor of about 4.5×10^5 using 2-aminothiophenol as a probing molecule. Xiong Y. and co-workers discovered that the hydroxyl end groups of poly(vinyl pyrrolidone)(PVP) could serve as a very mild reductant for kinetically controlled synthesis of Ag nanoplates,[124] and hydroxyl-terminated PVP is also a well-suited reductant for the aqueous synthesis of circular, triangular, and hexagonal nanoplates made of other noble metals including Pd, Au, and Pt. With sharp corners and edges, the triangular nanoplates are potentially useful as active substrates for SERS and related applications. Qin D. and co-workers performed a systematic investigation on the role of etching in the formation of Ag nanoplates during the reduction of $AgNO_3$ by poly(vinyl pyrrolidone)(PVP).[125] When the nanoplates with straight edges are transferred into ethanol and subjected to a solvothermal treatment, nanoplates with wavy edges and sharp corners can be obtained owing to etching on the edges. A comparison study indicates that Ag nanoplates with wavy edges and sharp corners were more active SERS substrates than those with straight and curved edges. In another report, Tan T. and co-workers employed a seed-mediated method to synthesize silver nanoplates with broad-tuning LSPR and high stability, and the LSPR peaks could be tuned in the range from 485 to ～1200 nm (Figure 9).[126] The SERS performance is largely dependent on the LSPR of the silver nanoplates at a given excitation wavelength, and specifically the Raman signals were greatly enhanced when the laser excitation line matched the peak position of LSPR band.

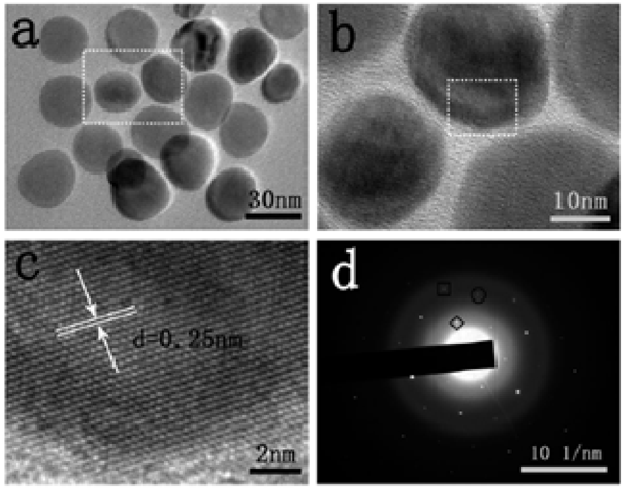

Figure 9. TEM images of Ag nanoplates with different magnifications (a and b); HRTEM images of silver nanoplates taken from the flat top face (c). Selected area electron diffraction (SAED) pattern (d) taken from a single nanoplate. (reprinted with permission from ref. 126. Copyright 2013)

4.2 Nanodisks

Recently, several reports have focused on the synthesis of noble metal nanodisks by various methods.[50, 135-140] Tang B. and co-workers had successfully prepared, in a large quantity, uniform and stable silver nanodisks by heat aging of silver nanoprisms.[135] The shape transformation from nanoprisms to nanodisks was caused by the difference in surface energy of the facets and the facet-selectivity of the citrate. The LSPR of the silver nanoplates could be tuned in a certain range in the heat-aging process. They then developed a simple and convenient method to transform silver nanoprisms into nanodisks by adding the chloride ions into the silver colloid.[136] The chloride ions could etch the corners and side faces of the silver nanoprism, and the resulting nanoparticles were disk-like in shape. The dissolved silver atoms would aggregate to form small silver clusters stabilized by the Cl^- and citrate ions. The as-prepared nanodisks showed higher SERS activity as compared to that of the original nanoprisms, which might be due to the existence of the silver cluster in the system of silver nanodisks.

4.3 Nanoprisms

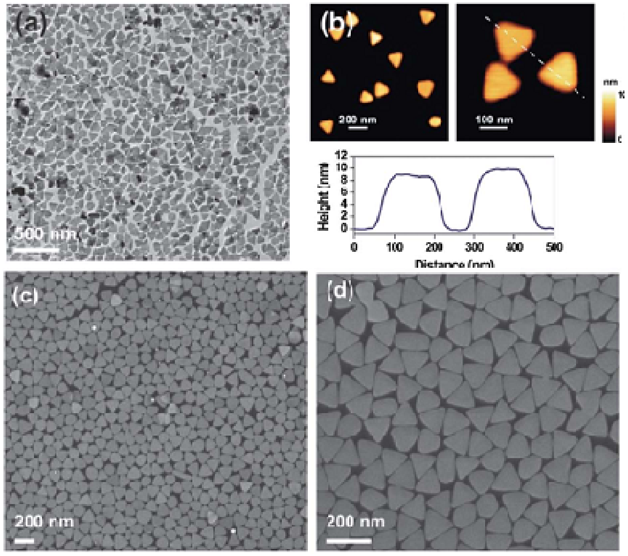

Figure 10. Characterizing the Au nanoprisms. (a) TEM image and (b) AFM images and cross-sectional height profiles of Au nanoprisms; (c) low and (d) high magnification of SEM images of the self-assembled Au nanoprisms monolayer by Langmuir-Schaefer assembly. (reprinted with permission from ref. 138. Copyright 2013)

Nanoprisms have attracted extensive research interest because of the unique optical properties that arise as a result of their localized surface plasmon resonance modes.[136] They have shown strong scattering and have been calculated to exhibit large local field enhancements due to their sharp tips. As a result of the highly advantageous properties, nanoprisms have a wide variety of applications, including their use as sensors in SERS.[130] Bae Y. and co-workers prepared the silver nanoprisms with anisotropic orientation by thermal synthetic method.[133] Almost the Ag nanoprisms were truncated with average edge length of 30±7 nm. The SERS properties of the assemblies were determined by 4-aminobenzenethiol (4-ABT) as a model compound. 4-ABT molecule adsorbed strongly on the Ag surface by forming an Ag-S bond and showed vibrational mode-selective SERS enhancement owing to the charge transfer from metal to molecule. Ciou S.-H. and co-workers had synthesized silver nanoprisms by photoreducing the silver ions by citrate. SERS signals of R6G had been observed in silver nanoprisms in the presence of KBr.[134] The silver nanoprisms have an average edge length of 70 ± 30 nm and thickness of about 10 ± 2 nm. The SERS intensity of R6G (4.5×10^{-9} M) in the silver nanoprisms was much stronger in contrast with the spherical nanoparticle, and the enhancement factor of the nanoprism is about 3.2×10^{5}. In Lin X. and co-workers' report, a scalable process was developed to fabricate large-area monolayer Au nanoprisms films at the air-water interface using the Langmuir-Schaefer technique.[133] The inter-prism gaps of the films can be tuned qualitatively through the introduction of dodecanethiol and oleylamine, and the near close-packed arrangement of the nanoprisms monolayers generates large numbers of hot spots in the 2D arrays, giving rise to strong SERS signals, which can be used for SERS applications in many fields (see Figure 10).

4.4 Nanostars

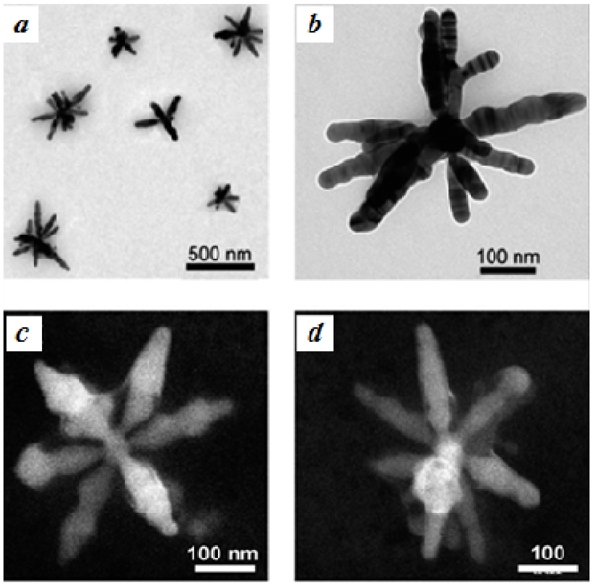

Figure 11. Micrographs of Ag nanostars obtained by (a and b) TEM and (c and d) SEM. (reprinted with permission from ref. 45. Copyright 2013)

Because of the extraordinary properties in the intensification of the EM field, star-shaped NPs or metal nanostars have shown promising applications in bioimaging and detection.[47] Recently, the synthesis of novel nanostars has been reported, and the most commonly nanostars are gold nanostars and silver nanostars. Gold nanostars ranging from 45 to 116 nm in size were synthesized in high yield by Khoury C.G. and co-workers, and the measured SERS enhancement factors suggest an interesting correlation between nanostar size and SERS effect. The enhancement factors were relatively consistent across different star samples, for instance, a factor of 5×10^{3} averaged over the 52 nm nanostars for 633-nm excitation.[47] Garcia-Leis A. and co-workers used a simple method consisting of the chemical reduction of Ag^{+} by neutral hydroxylamine, followed by a capping–reduction process induced by citrate to fabricate silver nanostars,[47] (Figure 11) which displayed a high performance in SERS applications. The effectiveness of these nanostars was probed by using the drug probenecid (PB), leading to intense SERS spectra without the addition of aggregation agents.

5. Three Dimensional Nanostructures

With increasing interest on the discovery of proper metal substrates for SERS-based applications, three-dimensional (3D) morphology control of metallic nanostructures to generate effective and adequate hot spots for creating strong and tunable electromagnetic field is gaining great attention.[53] Recently, 3D nanostructures such as nanocages[141-147], nanoflowers[52-58, 148-150], nanodendrites[151,152] and nanocaps[153,154] have been designed for SERS applications.

5.1 Nanocages

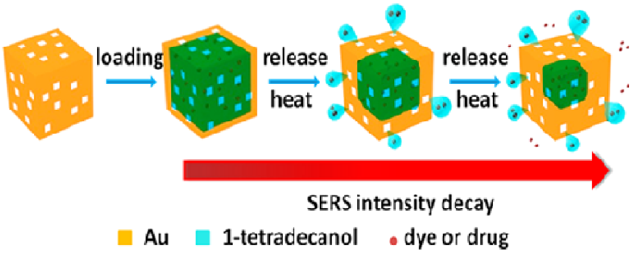

Figure 12. Scheme illustrating the loading of a gold nanocage with 1-tetradecanol and dye/drug followed by its release with external trigger. A decrease in the SERS intensity of dye/drug during its release can be employed to directly monitor the release process. (reprinted with permission from ref. 146. Copyright 2013)

Nanocages, a novel class of hollow plasmonic nanostructures, possess hollow interiors and porous walls. Nanocages made of noble metals are particularly attractive because of their strong scattering and absorption peaks in the near-infrared region known as surface plasmon resonance.[144] Recently, nanocages have been proved to be efficient carriers of chemotherapeutic drugs for targeted and triggered delivery and potentially used for SERS.[145] Metallic nanocages can be formed by depositing thin shells of a metal on silica or polymer beads followed by selective removal of the beads. More recently, a new method have been developed based on galvanic replacement reaction between Ag nanostructures and Au, Pt, or Pd compounds to fabricate nanocages characterized by single-crystal walls.[147] Tian L. and co-workers applied this method to prepare gold nanocages.[146] First, Ag nanocubes were synthesized by sulfide-mediated polyol synthesis method, and then Au nanocages were obtained by galvanic replacement of Ag nanocubes with gold using $HAuCl_4$. They employed SERS to noninvasively monitor the release of payload from nanocages. The large enhancement of electromagnetic field at the interior surface of nanocages enabled to monitor the controlled release of Raman-active cargo from nanocages. They used a biocompatible phasechange material, namely, 1-tetradecanol, as a "gate keeper" to control the release of cargo in response to an external stimulus. And the results showed that release process can be followed in situ using SERS without limitation (Figure 12). They demonstrated that SERS could serve as a noninvasive technique to monitor the release of Raman-active molecules such as dyes and drugs from plasmonic nanocages. It is reported that the photothermal (PT) effect occurs when a metal nanoparticle absorbs light and releases it as heat.[141] This heat can affect the molecules on the nanoparticle's surface and heat up the local environment. And both SERS and the PT effect share the same fundamental mechanism of plasmon excitation that generates strong local E-fields for SERS and heat for the PT effect which makes SERS a very simple and attractive technique for probing the PT effect. Rycenga M. and co-workers employed SERS as a sensitive tool to probe the PT effect, leading to direct examination of the heat generated at the nanocage's surface.[141] They had used 1-dodecanethiolate (1-DDT) SAM to probe the PT effect of Au-Ag nanocages. And the SERS measurements could quantify the temperature changes experienced by the 1-DDT SAMs on Au-Ag nanocages.

5.2 Nanoflowers

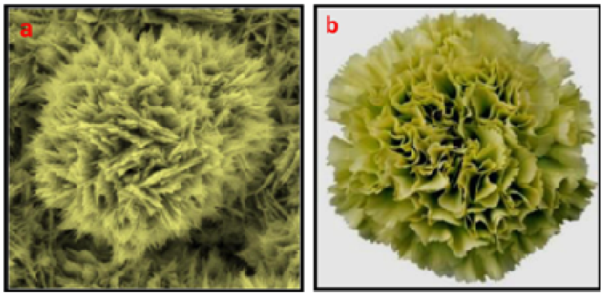

Figure 13. FESEM images of Au flower (a) and digital photograph of natural carnation flower (b). (reprinted with permission from ref. 53. Copyright 2012)

Recently, as the development of nanotechnology, different novel 3D nanostructures have been prepared. Among them, nanoflowers have attracted special interest due to pronounced electromagnetic field effect surrounding nanoflowers, which provide a new chance to extend the applications of nanocrystals in SERS.[55] Rosette-like Au nanoflowers were simply prepared by Shin H. S. and co-workers through one-pot reduction of the $AuCl_4^-$ precursor by 2-thiopheneacetic acid (2-TAA) without extra surface capping ligands at room temperature.[53] In this experiment, 2-TAA played a bifunctional role as both a reducing agent for the Au precursor and an effective surface-stabilizing agent during formation of Au nanostructures. Rosette-like Au nanoflowers were considered as superior SERS substrates because of sharp tips and nanogaps. Therefore, the potential of rosette-like Au nanoflowers as an SERS-active substrate were investigated by using two important biological staining agents, methylene blue (MB) and crystal violet (CV) which have been reported to give good quality Raman spectra, as probe molecules. And the rosette-like Au nanoflowers were considered to be good SERS substrates for MB and CV with the respective SERS enhancement factors of 2.6×10^8 and 8.8×10^5. Jena B.K. and co-workers had prepared branched silver nanoflowers by using a biofriendly molecule-rutin, which acts as a reducing/stabilizing agent.[149] The SERS activity of Ag nanoflowers was investigated with methylene blue (MB) as a probe molecule with the SERS enhancement of 2.4×10^6, which indicated the potential for the Ag nanoflowers used as SERS substrate. Highly branched Au nanoflowers with sharp tips have been synthesized in high yield by Pradhan M. and co-workers.[53] The Au nanoflowers were fabricated by galvanic exchange of polystyrene bead supported Cu (prepared by $NaBH_4$ reduction) nanoparticle with $HAuCl_4$ at about 90 °C. The prickly tips of the gold bearing enhanced field with a large number of embedded hot spots hidden within the oriented invited a probe molecule to show the enhancement even for a concentration of 4-mercaptopyridine (4-MPy) down to 10^{-12} mol dm^{-3}. The SERS results guarantee that the as-prepared naked AuF is an excellent and stable SERS substrate.

5.3 Nanodendrites

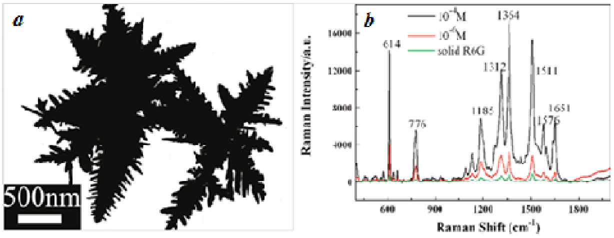

Figure 14. TEM (a) images of dendritic gold nanostructures and Raman spectrum of solid R6G and SERS spectra of R6G molecules adsorbed on the dendritic gold nanostructures (b). (reprinted with permission from ref. 152. Copyright 2011)

Nowadays, great efforts have been devoted to synthesize 3D shape-controlled nanostructures.[152] Besides nanocages and nanoflowers, other 3D nanostructures, such as nanodendrites, nanocaps, have been employed as SERS substrates. 3D dendritic gold nanostructures have been prepared by Huang D. and co-workers via an ultrafast one-step homogeneous solution method.[152] In this method, cationic surfactants, decane-1,10-bis(methylpyrrolidinium bromide) ([mpy-C_{10}-mpy]Br_2), were used as the capping agent and L-ascorbic acid (AA) was used as the reducing agent. The methylpyrrolidinium quaternary ammonium headgroups and bolaform nanostructures of the surfactants are the key factors for the formation of dendritic structures. With sharp corners, edges and nanoscale junctions, the as-prepared gold nanodendrites were investigated of SERS sensitivity by using Rhodamine 6G (R6G) as a model molecule. The SERS intensity increased greatly when the concentration of R6G increases from 1×10^{-6} M to 1×10^{-4} M (Figure 14). And the enhancement factor was calculated to be 2.52×10^4 when the concentration of R6G is 1×10^{-4} M, which showed potential application of nanodendrites in SERS based technology. Lu G. and co-workers also prepared 3D gold nanodendrites at room temperature through an aqueous/organic interfacial reaction of hydrogen tetrachloroaurate ($HAuCl_4$, in aqueous phase) and 3,4-ethylenedioxythiophene (EDOT, in organic phase).[151] They found that the as-prepared 3D gold nanodendrites could be used as SERS substrates. 4-mercaptopyridine (4MP) was used as a molecule probe. The 3D gold nanodentrites exhibited much higher surface enhancement than those of conventional electrochemically roughed gold surfaces and gold nanorods. And The enhancement factor of the 3D gold nanodentrites substrate was measured to be $(1.9\pm0.4)\times10^6$, and the limit of detection (LOD) was determined to be lower than 1×10^{-10} M.

6. Conclusions and Outlook

The properties of high selectivity and sensitivity have made SERS one of the most promising analytical techniques for biological and chemical sciences. Significant progress has been made on the synthesis of nanostructured materials. Various nanostructured materials have been designed and prepared for SERS. The characteristics of nanostructured materials, such as their size distribution, geometry, chemical composition, and surface chemistry have a great influence on the SERS enhancement factors. By comparison, we can easily conclude that nanostructured materials with complex structures like rich sharp edges, junctions and narrow gaps, will have much higher SERS enhancement factors.

Most SERS-active nanostructured materials are noble metallic materials, like gold, silver and copper. However, future efforts should be made on the synthesis of other more novel materials, such as other metal, metal oxide, semiconductor materials, graphene, and hybrid nanostructures. The nanostructures listed in this review are thought to be typically in noble metal nanoparticles, 1D nanostructures, 2D nanostructures and 3D nanostructures. In addition to these nanostructures, novel approaches should be exploited to design and create even more efficient SERS-active nanostructures, which are rarely utilized as SERS-active media in current studies.

Acknowledgements

This work was supported by the Natural Science Foundation of China (Nos. 21371174) and the National Science & Technology Pillar Program (Grant 2012BAJ24B02).

Notes and references

[a]*Institute of Intelligent Machines, Chinese Academy of Sciences, Hefei, Anhui, 230031, China. E-mail: cljiang@iim.ac.cn*
[b]*School of Chemistry and Chemical Engineering, Hefei University of Technology and Anhui Key Laboratory of Controllable Chemical Reaction & Material Chemical Engineering, Hefei, Anhui, 230009, China.*
E-mail: shmyu@hfut.edu.cn

1 R. A. Alvarez-Puebla and L. M. Liz-Marzan, *Angew Chem Int Ed Engl*, 2012, **51**, 11214-11223.
2 H. Ko, S. Singamaneni and V. V. Tsukruk, *Small*, 2008, **4**, 1576-1599.
3 J. Kneipp, H. Kneipp and K. Kneipp, *Chem. Soc. Rev.*, 2008, **37**, 1052-1060.
4 N. P. Pieczonka and R. F. Aroca, *Chem. Soc. Rev.*, 2008, **37**, 946-954.
5 V. Uzayisenga, X. D. Lin, L. M. Li, J. R. Anema, Z. L. Yang, Y. F. Huang, H. X. Lin, S. B. Li, J. F. Li and Z. Q. Tian, *Langmuir*, 2012, **28**, 9140-9146.
6 Y. Wang, B. Yan and L. Chen, *Chem. Rev. (Washington, DC, U. S.)*, 2013, **113**, 1391-1428.
7 R. A. Halvorson and P. J. Vikesland, *Environ. Sci. Technol.*, 2010, **44**, 7749-7755.
8 C. L. Haynes, A. D. McFarland and R. P. V. Duyne, *Anal. Chem.*, 2005, **77**, 338 A-346 A.
9 I. E. Pavel, K. S. Alnajjar, J. L. Monahan, A. Stahler, N. E. Hunter, K. M. Weaver, J. D. Baker, A. J. Meyerhoefer and D. A. Dolson, *J. Chem. Educ.*, 2012, **89**, 286-290.
10 Z.-Q. Tian, B. Ren and D.-Y. Wu, *The Journal of Physical Chemistry B*, 2002, **106**, 9463-9483.
11 Y.-C. Yang, T.-K. Huang, Y.-L. Chen, J.-Y. Mevellec, S. Lefrant, C.-Y. Lee and H.-T. Chiu, *The Journal of Physical Chemistry C*, 2011, **115**, 1932-1939.
12 E. D. Diebold, N. H. Mack, S. K. Doorn and E. Mazur, *Langmuir*, 2009, **25**, 1790-1794.
13 K. Ikeda, S. Suzuki and K. Uosaki, *J. Am. Chem. Soc.*, 2013, **135**, 17387-17392.
14 H. L. Liu, Z. L. Yang, L. Y. Meng, Y. D. Sun, J. Wang, L. B. Yang, J. H. Liu and Z. Q. Tian, *J. Am. Chem. Soc.*, 2014, **136**, 5332-5341.
15 X. H. Tang, W. Y. Cai, L. B. Yang and J. H. Liu, *Nanoscale*, 2014, **6**, 8612-8616.
16 L. B. Yang, H. L. Liu, J. Wang, F. Zhou, Z. Q. Tian and J. H. Liu, *Chem. Commun.*, 2011, **47**, 3583-3585.
17 X. H. Li, G. Y. Chen, L. B. Yang, Z. Jin and J. H. Liu, *Adv.Funct. Mater.*, 2010, **20**, 2815-2824.
18 L. B. Yang, L. A. Ma, G. Y. Chen, J. H. Liu and Z. Q. Tian, *Chem. Eur. J.*, 2010, **16**, 12683-12693.
19 C. Steuwe, C. F. Kaminski, J. J. Baumberg and S. Mahajan, *Nano Lett.*, 2011, **11**, 5339-5343.
20 J. Zhang, X. Li, X. Sun and Y. Li, *The Journal of Physical Chemistry B*, 2005, **109**, 12544-12548.
21 L. Chen, Z. Li, Y. Meng, M. Lu, Z. Wang and R.-Q. Zhang, *The Journal of Physical Chemistry C*, 2013, **117**, 12544-12551.
22 J. Kumar and K. G. Thomas, *The Journal of Physical Chemistry Letters*, 2011, **2**, 610-615.
23 E. J. Titus, M. L. Weber, S. M. Stranahan and K. A. Willets, *Nano Lett.*, 2012, **12**, 5103-5110.
24 B. Yan, A. Thubagere, W. R. Premasiri, L. D. Ziegler, L. Dal Negro and B. M. Reinhard, *ACS Nano*, 2009, **3**, 1190-1202.
25 M. J. Banholzer, J. E. Millstone, L. Qin and C. A. Mirkin, *Chem. Soc. Rev.*, 2008, **37**, 885.
26 N. Mirsaleh-Kohan, V. Iberi, P. D. Simmons, N. W. Bigelow, A. Vaschillo, M. M. Rowland, M. D. Best, S. J. Pennycook, D. J. Masiello, B. S. Guiton and J. P. Camden, *The Journal of Physical Chemistry Letters*, 2012, **3**, 2303-2309.
27 W. E. Doering and S. Nie, *The Journal of Physical Chemistry B*, 2002, **106**, 311-317.
28 W. Leng and P. J. Vikesland, *Anal. Chem.*, 2013, **85**, 1342-1349.
29 G. Kumari and C. Narayana, *The Journal of Physical Chemistry Letters*, 2012, **3**, 1130-1135.
30 M. A. Mahmoud, D. O'Neil and M. A. El-Sayed, *Chem. Mater.*, 2014, **26**, 44-58.
31 H.-J. Yang, C.-Y. Chen, F.-W. Yuan and H.-Y. Tuan, *The Journal of Physical Chemistry C*, 2013, **117**, 21955-21964.
32 J. Qiu, Y. C. Wu, Y. C. Wang, M. H. Engelhard, L. McElwee-White and W. D. Wei, *J. Am. Chem. Soc.*, 2013, **135**, 38-41.
33 S. S. Dasary, A. K. Singh, D. Senapati, H. Yu and P. C. Ray, *J. Am. Chem. Soc.*, 2009, **131**, 13806-13812.
34 A.-X. Yin, W.-C. Liu, J. Ke, W. Zhu, J. Gu, Y.-W. Zhang and C.-H. Yan, *J. Am. Chem. Soc.*, 2012, **134**, 20479-20489.
35 M. G. Blaber, A.-I. Henry, J. M. Bingham, G. C. Schatz and R. P. Van Duyne, *The Journal of Physical Chemistry C*, 2012, **116**, 393-403.
36 W. J. Stark, *Angew Chem Int Ed Engl*, 2011, **50**, 1242-1258.
37 K. V. Kong, Z. Lam, W. D. Goh, W. K. Leong and M. Olivo, *Angew Chem Int Ed Engl*, 2012, **51**, 9796-9799.
38 C. Jiang, R. Liu, G. Han and Z. Zhang, *Chem. Commun.*, 2013, **49**, 6647-6649.
39 L. Zhang, C. Jiang and Z. Zhang, *Nanoscale*, 2013, **5**, 3773-3779.
40 C. C. Chang, K. H. Yang, Y. C. Liu, T. C. Hsu and F. D. Mai, *ACS Appl. Mater. Interfaces*, 2012, **4**, 4700-4707.
41 D. Y. Wu, J. F. Li, B. Ren and Z. Q. Tian, *Chem. Soc. Rev.*, 2008, **37**, 1025-1041.
42 S. Su, W. Wu, J. Gao, J. Lu and C. Fan, *J. Mater. Chem.*, 2012, **22**, 18101.
43 M. Rycenga, P. H. Camargo, W. Li, C. H. Moran and Y. Xia, *J Phys Chem Lett*, 2010, **1**, 696-703.
44 C. P. Shaw, M. Fan, C. Lane, G. Barry, A. I. Jirasek and A. G. Brolo, *The Journal of Physical Chemistry C*, 2013, **117**, 16596-16605.
45 A. Garcia-Leis, J. V. Garcia-Ramos and S. Sanchez-Cortes, *The Journal of Physical Chemistry C*, 2013, **117**, 7791-7795.
46 M. Mueller, M. Tebbe, D. V. Andreeva, M. Karg, R. A. Alvarez Puebla, N. Pazos Perez and A. Fery, *Langmuir*, 2012, **28**, 9168-9173.
47 C. G. Khoury and T. Vo-Dinh, *The Journal of Physical Chemistry C*, 2008, **112**, 18849-18859.
48 C. Liusman, H. Li, G. Lu, J. Wu, F. Boey, S. Li and H. Zhang, *The Journal of Physical Chemistry C*, 2012, **116**, 10390-10395.

49 S. Tripathy, R. Marty, V. K. Lin, S. L. Teo, E. Ye, A. Arbouet, L. Saviot, C. Girard, M. Y. Han and A. Mlayah, *Nano Lett.*, 2011, **11**, 431-437.
50 X. Jiang, Z. Jiang, T. Xu, S. Su, Y. Zhong, F. Peng, Y. Su and Y. He, *Anal. Chem.*, 2013, **85**, 2809-2816.
51 H. S. Shin, J. Y. Hong and S. Huh, *ACS Appl. Mater. Interfaces*, 2013, **5**, 1429-1435.
52 W. Jia, J. Li, G. Lin and L. Jiang, *Cryst. Growth Des.*, 2011, **11**, 3822-3827.
53 M. Pradhan, J. Chowdhury, S. Sarkar, A. K. Sinha and T. Pal, *The Journal of Physical Chemistry C*, 2012, **116**, 24301-24313.
54 H.-Y. Hsieh, J.-L. Xiao, C.-H. Lee, T.-W. Huang, C.-S. Yang, P.-C. Wang and F.-G. Tseng, *The Journal of Physical Chemistry C*, 2011, **115**, 16258-16267.
55 J. Wang, G. Duan, Y. Li, G. Liu, Z. Dai, H. Zhang and W. Cai, *Langmuir*, 2013, **29**, 3512-3517.
56 L. Zhong, X. Zhai, X. Zhu, P. Yao and M. Liu, *Langmuir*, 2010, **26**, 5876-5881.
57 E. Hutter and J. H. Fendler, *Adv. Mater. (Weinheim, Ger.)*, 2004, **16**, 1685-1706.
58 J. M. McLellan, A. Siekkinen, J. Chen and Y. Xia, *Chem. Phys. Lett.*, 2006, **427**, 122-126.
59 T. A. Laurence, G. Braun, C. Talley, A. Schwartzberg, M. Moskovits, N. Reich and T. Huser, *J. Am. Chem. Soc.*, 2008, **131**, 162-169.
60 W. Premasiri, D. Moir, M. Klempner, N. Krieger, G. Jones and L. Ziegler, *The Journal of Physical Chemistry B*, 2005, **109**, 312-320.
61 L. Li, U. Steiner and S. Mahajan, *Nano Lett.*, 2014, **14**, 495-498.
62 L. Sun, D. Zhao, M. Ding, H. Zhao, Z. Zhang, B. Li and D. Shen, *Appl. Surf. Sci.*, 2012, **258**, 7813-7819.
63 J. M. Kohler, A. Marz, J. Popp, A. Knauer, I. Kraus, J. Faerber and C. Serra, *Anal. Chem.*, 2013, **85**, 313-318.
64 Y. Han, S. Liu, B. Liu, C. Jiang and Z. Zhang, *RSC Advances*, 2014, **4**, 2776.
65 S. Murphy, L. Huang and P. V. Kamat, *The Journal of Physical Chemistry C*, 2013, **117**, 4740-4747.
66 Y. Liu, L. Liu and R. Guo, *Langmuir*, 2010, **26**, 13479-13485.
67 E. Hariprasad and T. P. Radhakrishnan, *Langmuir*, 2013, **29**, 13050-13057.
68 K. Y. van Berkel, A. M. Piekarski, P. H. Kierstead, E. D. Pressly, P. C. Ray and C. J. Hawker, *Macromolecules*, 2009, **42**, 1425-1427.
69 J.-M. Li, W.-F. Ma, C. Wei, J. Guo, J. Hu and C.-C. Wang, *J. Mater. Chem.*, 2011, **21**, 5992.
70 X. Su, J. Zhang, L. Sun, T.-W. Koo, S. Chan, N. Sundararajan, M. Yamakawa and A. A. Berlin, *Nano Lett.*, 2005, **5**, 49-54.
71 T. I. Abdullin, O. V. Bondar, Y. G. Shtyrlin, M. Kahraman and M. Culha, *Langmuir*, 2010, **26**, 5153-5159.
72 J. Ye, F. Wen, H. Sobhani, J. B. Lassiter, P. Van Dorpe, P. Nordlander and N. J. Halas, *Nano Lett.*, 2012, **12**, 1660-1667.
73 J. C. Fraire, L. A. Pérez and E. A. Coronado, *The Journal of Physical Chemistry C*, 2013, **117**, 23090-23107.
74 I. Chakraborty, S. Bag, U. Landman and T. Pradeep, *The Journal of Physical Chemistry Letters*, 2013, **4**, 2769-2773.
75 A. W. Wark, R. J. Stokes, S. B. Darby, W. E. Smith and D. Graham, *The Journal of Physical Chemistry C*, 2010, **114**, 18115-18120.
76 L. Sun, Y. Song, L. Wang, C. Guo, Y. Sun, Z. Liu and Z. Li, *The Journal of Physical Chemistry C*, 2008, **112**, 1415-1422.
77 L. O. Brown and S. K. Doorn, *Langmuir*, 2008, **24**, 2277-2280.
78 K. L. Wustholz, A.-I. Henry, J. M. McMahon, R. G. Freeman, N. Valley, M. E. Piotti, M. J. Natan, G. C. Schatz and R. P. V. Duyne, *J. Am. Chem. Soc.*, 2010, **132**, 10903-10910.
79 W. J. Cho, Y. Kim and J. K. Kim, *ACS Nano*, 2012, **6**, 249-255.
80 R. Liu, J.-f. Liu, X.-x. Zhou, M.-T. Sun and G.-b. Jiang, *Anal. Chem.*, 2011, **83**, 9131-9137.
81 S. Coskun, B. Aksoy and H. E. Unalan, *Cryst. Growth Des.*, 2011, **11**, 4963-4969.
82 S. Chang, H. Ko, R. Gunawidjaja and V. V. Tsukruk, *The Journal of Physical Chemistry C*, 2011, **115**, 4387-4394.
83 M. Chen, C. Wang, X. Wei and G. Diao, *The Journal of Physical Chemistry C*, 2013, **117**, 13593-13601.
84 C. Xu, H. Geng, R. Bennett, D. A. Clayton and S. Pan, *The Journal of Physical Chemistry C*, 2013, **117**, 1849-1856.
85 M. S. Goh, Y. H. Lee, S. Pedireddy, I. Y. Phang, W. W. Tjiu, J. M. R. Tan and X. Y. Ling, *Langmuir*, 2012, **28**, 14441-14449.
86 P. Mohanty, I. Yoon, T. Kang, K. Seo, K. S. Varadwaj, W. Choi, Q.-H. Park, J. P. Ahn, Y. D. Suh and H. Ihee, *J. Am. Chem. Soc.*, 2007, **129**, 9576-9577.
87 X. Li, M. Cao, H. Zhang, L. Zhou, S. Cheng, J.-L. Yao and L.-J. Fan, *J. Colloid Interface Sci.*, 2012, **382**, 28-35.
88 H. Zhu, M. Du, M. Zhang, P. Wang, S. Bao, M. Zou, Y. Fu and J. Yao, *Biosensors and Bioelectronics*, 2014, **54**, 91-101.
89 C. M. Payne, L. J. E. Anderson and J. H. Hafner, *The Journal of Physical Chemistry C*, 2013, **117**, 4734-4739.
90 Z. Yang, K. T. Nguyen, H. Chen, H. Qian, L. P. Fernando, K. A. Christensen and J. N. Anker, *The Journal of Physical Chemistry Letters*, 2011, **2**, 1742-1746.
91 J. Bai, Y. Qin, C. Jiang and L. Qi, *Chem. Mater.*, 2007, **19**, 3367-3369.
92 R. Venugopal, P.-I. Lin, C.-C. Liu and Y.-T. Chen, *J. Am. Chem. Soc.*, 2005, **127**, 11262-11268.
93 N. Zhao, Y. Wei, N. Sun, Q. Chen, J. Bai, L. Zhou, Y. Qin, M. Li and L. Qi, *Langmuir*, 2008, **24**, 991-998.
94 Y. Chen, S. Milenkovic and A. W. Hassel, *Nano Lett.*, 2008, **8**, 737-742.
95 R. Contreras-Caceres, C. Dawson, P. Formanek, D. Fischer, F. Simon, A. Janke, P. Uhlmann and M. Stamm, *Chem. Mater.*, 2013, **25**, 158-169.
96 A. M. Gabudean, M. Focsan and S. Astilean, *The Journal of Physical Chemistry C*, 2012, **116**, 12240-12249.
97 B. N. Khlebtsov, V. A. Khanadeev, M. Y. Tsvetkov, V. N. Bagratashvili and N. G. Khlebtsov, *The Journal of Physical Chemistry C*, 2013, **117**, 23162-23171.
98 S. Guo, S. Dong and E. Wang, *Crystal Growth and Design*, 2008, **9**, 372-377.
99 Y.-J. Liu, H. Y. Chu and Y.-P. Zhao, *The Journal of Physical Chemistry C*, 2010, **114**, 8176-8183.
100 L. Vigderman and E. R. Zubarev, *Langmuir*, 2012, **28**, 9034-9040.
101 G. H. Gu and J. S. Suh, *Langmuir*, 2008, **24**, 8934-8938.
102 J. Zhu, J.-J. Li and J.-W. Zhao, *The Journal of Physical Chemistry C*, 2013, **117**, 584-592.
103 T. Fujimori, K. Urita, T. Ohba, H. Kanoh and K. Kaneko, *J. Am. Chem. Soc.*, 2010, **132**, 6764-6767.
104 P. Leyton, J. S. Gómez-Jeria, S. Sanchez-Cortes, C. Domingo and M. Campos-Vallette, *The Journal of Physical Chemistry B*, 2006, **110**, 6470-6474.
105 M. Dresselhaus, G. Dresselhaus and A. Jorio, *The Journal of Physical Chemistry C*, 2007, **111**, 17887-17893.
106 Y.-C. Chen, R. J. Young, J. V. Macpherson and N. R. Wilson, *The Journal of Physical Chemistry C*, 2007, **111**, 16167-16173.
107 S. Alidori, K. Asqiriba, P. Londero, M. Bergkvist, M. Leona, D. A. Scheinberg and M. R. McDevitt, *The Journal of Physical Chemistry C*, 2013, **117**, 5982-5992.
108 P. Goldberg-Oppenheimer, T. Hutter, B. Chen, J. Robertson, S. Hofmann and S. Mahajan, *The Journal of Physical Chemistry Letters*, 2012, **3**, 3486-3492.
109 Y. Sun, K. Liu, J. Miao, Z. Wang, B. Tian, L. Zhang, Q. Li, S. Fan and K. Jiang, *Nano Lett.*, 2010, **10**, 1747-1753.
110 J. E. Bohn, P. G. Etchegoin, E. C. Le Ru, R. Xiang, S. Chiashi and S. Maruyama, *ACS Nano*, 2010, **4**, 3466-3470.
111 M. S. Dresselhaus, *ACS Nano*, 2010, **4**, 4344-4349.
112 K. Kneipp, H. Kneipp, M. S. Dresselhaus and S. Lefrant, *Philosophical Transactions of the Royal Society of London. Series A: Mathematical, Physical and Engineering Sciences*, 2004, **362**, 2361-2373.
113 P. Corio, S. Brown, A. Marucci, M. Pimenta, K. Kneipp, G. Dresselhaus and M. Dresselhaus, *Physical Review B*, 2000, **61**, 13202.
114 Y. Liu, Z. Ma and S. Ramakrishna, *Current Nanoscience*, 2006, **2**, 71-78.
115 S. Shanmukh, L. Jones, J. Driskell, Y. Zhao, R. Dluhy and R. A. Tripp, *Nano Lett.*, 2006, **6**, 2630-2636.

116 J. V. Jokerst, A. J. Cole, D. Van de Sompel and S. S. Gambhir, *ACS Nano*, 2012, **6**, 10366-10377.

117 Z. W. Pan, Z. R. Dai and Z. L. Wang, *Science*, 2001, **291**, 1947-1949.

118 D. Jana, A. Mandal and G. De, *ACS Appl. Mater. Interfaces*, 2012, **4**, 3330-3334.

119 G. Zhan, L. Ke, Q. Li, J. Huang, D. Hua, A.-R. Ibrahim and D. Sun, *Ind. Eng. Chem. Res.*, 2012, **51**, 15753-15762.

120 F. Pashaee, R. Hou, P. Gobbo, M. S. Workentin and F. Lagugné-Labarthet, *The Journal of Physical Chemistry C*, 2013, **117**, 15639-15646.

121 J. Roh, J. Yi and Y. Kim, *Langmuir*, 2010, **26**, 11621-11623.

122 X. Jiang, Q. Zeng and A. Yu, *Langmuir*, 2007, **23**, 2218-2223.

123 X. Zou and S. Dong, *The Journal of Physical Chemistry B*, 2006, **110**, 21545-21550.

124 Y. Xiong, I. Washio, J. Chen, H. Cai, Z.-Y. Li and Y. Xia, *Langmuir*, 2006, **22**, 8563-8570.

125 Y. Yang, X. L. Zhong, Q. Zhang, L. G. Blackstad, Z. W. Fu, Z. Y. Li and D. Qin, *Small*, 2014, **10**, 1430-1437.

126 T. Tan, C. Tian, Z. Ren, J. Yang, Y. Chen, L. Sun, Z. Li, A. Wu, J. Yin and H. Fu, *Phys. Chem. Chem. Phys.*, 2013, **15**, 21034-21042.

127 C.-M. Tsai, M.-S. Hsu, J.-C. Chen and C.-L. Huang, *The Journal of Physical Chemistry C*, 2012, **116**, 461-467.

128 E. Antoniou, P. Voudouris, A. Larsen, B. Loppinet, D. Vlassopoulos, I. Pastoriza-Santos and L. M. Liz-Marzán, *The Journal of Physical Chemistry C*, 2012, **116**, 3888-3896.

129 B. Pelaz, V. Grazu, A. Ibarra, C. Magen, P. del Pino and J. M. de la Fuente, *Langmuir*, 2012, **28**, 8965-8970.

130 L. Liu and T. L. Kelly, *Langmuir*, 2013, **29**, 7052-7060.

131 G. K. Joshi, K. N. Blodgett, B. B. Muhoberac, M. A. Johnson, K. A. Smith and R. Sardar, *Nano Lett.*, 2014, **14**, 532-540.

132 J. Nelayah, M. Kociak, O. Stephan, N. Geuquet, L. Henrard, F. J. Garcia de Abajo, I. Pastoriza-Santos, L. M. Liz-Marzan and C. Colliex, *Nano Lett.*, 2010, **10**, 902-907.

133 Y. Bae, N. H. Kim, M. Kim, K. Y. Lee and S. W. Han, *J. Am. Chem. Soc.*, 2008, **130**, 5432-5433.

134 S.-H. Ciou, Y.-W. Cao, H.-C. Huang, D.-Y. Su and C.-L. Huang, *The Journal of Physical Chemistry C*, 2009, **113**, 9520-9525.

135 B. Tang, J. An, X. Zheng, S. Xu, D. Li, J. Zhou, B. Zhao and W. Xu, *The Journal of Physical Chemistry C*, 2008, **112**, 18361-18367.

136 B. Tang, S. Xu, J. An, B. Zhao and W. Xu, *The Journal of Physical Chemistry C*, 2009, **113**, 7025-7030.

137 S. Chen, Z. Fan and D. L. Carroll, *The Journal of Physical Chemistry B*, 2002, **106**, 10777-10781.

138 Y. H. Lee, C. K. Lee, B. Tan, J. M. R. Tan, I. Y. Phang and X. Y. Ling, *Nanoscale*, 2013, **5**, 6404-6412.

139 M. Maillard, P. Huang and L. Brus, *Nano Lett.*, 2003, **3**, 1611-1615.

140 M. J. Banholzer, K. D. Osberg, S. Li, B. F. Mangelson, G. C. Schatz and C. A. Mirkin, *ACS Nano*, 2010, **4**, 5446-5452.

141 I. Zoric, M. Zach, B. Kasemo and C. Langhammer, *ACS Nano*, 2011, **5**, 2535-2546.

142 M. Rycenga, Z. Wang, E. Gordon, C. M. Cobley, A. G. Schwartz, C. S. Lo and Y. Xia, *Angew Chem Int Ed Engl*, 2009, **48**, 9924-9927.

143 J.-W. Liaw, J.-C. Cheng, C. Ma and R. Zhang, *The Journal of Physical Chemistry C*, 2013, DOI: 10.1021/jp403100m, 130916070600000.

144 J. Fang, S. Liu and Z. Li, *Biomaterials*, 2011, **32**, 4877-4884.

145 S. E. Skrabalak, J. Chen, Y. Sun, X. Lu, L. Au, C. M. Cobley and Y. Xia, *Acc. Chem. Res.*, 2008, **41**, 1587-1595.

146 L. Tian, N. Gandra and S. Singamaneni, *ACS Nano*, 2013, **7**, 4252-4260.

147 J. Chen, J. M. McLellan, A. Siekkinen, Y. Xiong, Z.-Y. Li and Y. Xia, *J. Am. Chem. Soc.*, 2006, **128**, 14776-14777.

148 H. Savaloni and R. Babaei, *Appl. Surf. Sci.*, 2013, **280**, 439-445.

149 B. K. Jena, B. Mishra and S. Bohidar, *The Journal of Physical Chemistry C*, 2009, **113**, 14753-14758.

150 S. Prabakar, C. W. Bumby and R. D. Tilley, *Chem. Mater.*, 2009, **21**, 1725-1730.

151 G. Lu, C. Li and G. Shi, *Chem. Mater.*, 2007, **19**, 3433-3440.

152 D. Huang, X. Bai and L. Zheng, *The Journal of Physical Chemistry C*, 2011, **115**, 14641-14647.

153 Y. Yang, T. Qiu, Z. Liu, Q. Hao, X. Lang, Q. Xu, G. Huang and P. K. Chu, *Appl. Surf. Sci.*, 2013, **280**, 343-348.

154 X. Lang, T. Qiu, W. Zhang, Y. Yin and P. K. Chu, *The Journal of Physical Chemistry C*, 2011, **115**, 24328-24333.

Author Information

Xiaochun Chen received his BS degree from Hefei University of Technology in China in 2013. He is currently a master student with Professor Shaoming Yu at Hefei University of Technology. His research interests focus on preparation of functional nanomaterials and their application in environmental analysis.

Changlong Jiang was born in Anhui, China. He received his PhD degree from the Department of Chemistry, University of Science &Technology of China in 2006. He moved to Japan afterwards and worked with Professor Kunihito Koumoto at Nagoya University, and then joined the group of Professor Xiaogang Liu at National University of Singapore as a research scientist. Since 2010, He is an associate professor at Institute of Intelligent Machines, Chinese Academy of Sciences. His current research is focused on nanostructured materials, nanosensors, and nanoscale spectroscopic methods at the frontiers of environment and nano-analysis.

Shao-Ming Yu received his BE degree (1983) from the Department of Chemical Engineering, Hefei University of Technology and ME degree (1988) from the Department of Chemistry, East China University of Science and Technology. Then, he began his academic career at School of Chemical Engineering, Hefei University of Technology. Since 1999, he has been a full professor. His research interests involve preparation of functional nanomaterials and their application in catalysis, adsorption and chemical analysis.

Table of contents entry

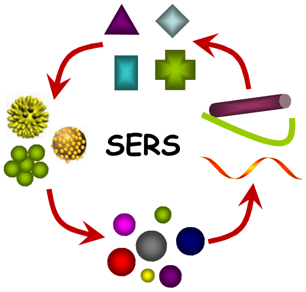

This highlight summarizes current advances on the design and the employment of nanostructured materials in SERS substrates especially from the point of dimensional view. We will then talk about synthesis methods and the novel properties of these nanostructured materials with their potential applications in SERS.